Inorganic Chemistry

Article

pubs.acs.org/IC

Thermal and Photochemical Reactivity of Manganese Tricarbonyl and Tetracarbonyl Complexes with a Bulky Diazabutadiene Ligand

Veeranna Yempally,[†] Samuel J. Kyran,[‡] Rajesh K. Raju,[†] Wai Yip Fan,[§] Edward N. Brothers,[†] Donald J. Darensbourg,*[,‡] and Ashfaq A. Bengali*[,†]

[†]Department of Chemistry, Texas A&M University at Qatar, Doha, Qatar

[§]Department of Chemistry, National University of Singapore, Kent Ridge, Singapore 119077

[‡]Department of Chemistry, Texas A&M University, College Station, Texas 77843, United States

Supporting Information

ABSTRACT: The manganese tricarbonyl complex *fac*-Mn(Br)(CO)$_3$(^{i}Pr$_2$Ph-DAB) (**1**) [^{i}Pr$_2$Ph-DAB = (*N*,*N*′-bis(2,6-diisopropylphenyl)-1,4-diaza-1,3-butadiene)] was synthesized from the reaction of Mn(CO)$_5$Br with the sterically encumbered DAB ligand. Compound **1** exhibits rapid CO release under low power visible light irradiation (560 nm) suggesting its possible use as a photoCORM. The reaction of compound **1** with TlPF$_6$ in the dark afforded the manganese(I) tetracarbonyl complex, [Mn(CO)$_4$(^{i}Pr$_2$Ph-DAB)][PF$_6$] (**2**). While **2** is comparatively more stable than **1** in light, it demonstrates high thermal reactivity such that dissolution in CH$_3$CN or THF at room temperature results in rapid CO loss and formation of the respective solvate complexes. This unusual reactivity is due to the large steric profile of the DAB ligand which results in a weak Mn−CO binding interaction.

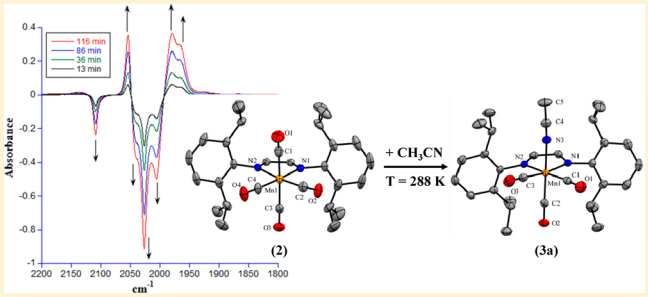

INTRODUCTION

Transition metal complexes with 1,4-diaza-1,3-butadiene (DAB) ligands bearing bulky aryl or alkyl groups on the nitrogen atoms have garnered much attention owing to their unusual oxidation state at the metal center and easily tunable stereoelectronic properties.[1] Low lying and long-lived MLCT excited states[2] and excellent coordination properties[3] are some of the key advantages of DAB ligands over conventional phosphine ligands.[4] Unusual electron donor and acceptor properties coupled with tunable absorption in the visible region allow metal-DAB complexes to be used in the preparation of photoactive materials[5] and in olefin polymerization chemistry.[6] Over the past few decades, several studies aimed at exploring the potential application of [MX(CO)$_n$(DAB)] (M = Ru or Re and X = halide or metal) compounds in the electrocatalytic reduction of CO$_2$ and in the synthesis of photoluminescent materials have been conducted.[7,8]

While a considerable number of reports have been published on the photoreactivity of [MnX(CO)$_3$(α-diimine)] (X = Br, Cl) complexes,[9] less is known for DAB based manganese tricarbonyl complexes with bulky aryl substituents on the nitrogen atoms.[10] Manganese tricarbonyl complexes have recently received much attention in the field of CO releasing molecules (CORMs).[11] CO gas is known to dilate blood vessels in a manner similar to nitric oxide and has been shown to possess anti-inflammatory and anti-apoptotic properties.[11b] Metal carbonyl complexes can be used as CO carriers, thus circumventing the inherent toxicity associated with CO inhalation.[11a] An important consideration in the design of these molecules is the facility with which they release CO either thermally or photochemically under visible light irradiation (photoCORMs). Several strategies have been adopted to improve the performance of metal carbonyl complexes in this respect. The use of sterically encumbered bulky chelating ligands for the activation of small molecules and C−H bonds has been successfully employed thus far,[1b,c,12] but extending the same strategy for CORM synthesis is largely unexplored and needs attention.

To ascertain the impact of bulky DAB ligands upon the properties of the corresponding manganese carbonyl complexes, the thermal and photochemical reactivity of the sterically encumbered *fac*-Mn(Br)(CO)$_3$(^{i}Pr$_2$Ph-DAB) (**1**) [^{i}Pr$_2$Ph-DAB = (*N*,*N*′-bis(2,6-di-isopropylphenyl)-1,4-diaza-1,3-butadiene)] and related cationic complexes is reported in this study (Figure 1). These complexes exhibit interesting reactivity including efficient thermal and photochemical CO loss. As such, the present findings suggest a role for steric manipulation of ligand characteristics in the design of CORMs. The experimental results were found to be consistent with theoretical calculations using DFT.

Received: January 6, 2014
Published: April 1, 2014

   dx.doi.org/10.1021/ic500025k | *Inorg. Chem.* 2014, 53, 4081−4088

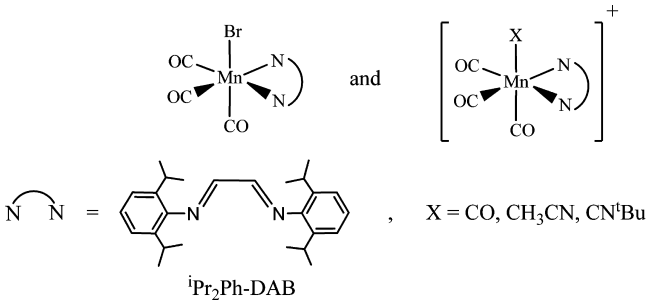

Figure 1. Molecular structures of the synthesized complexes.

EXPERIMENTAL SECTION

General. Unless otherwise stated, all experiments were performed in the absence of light. Anhydrous solvents and Schlenk techniques were used for the synthesis of all complexes. Manganese pentacarbonyl bromide ($Mn(CO)_5Br$) and thallium hexafluorophosphate ($TlPF_6$) were purchased from Strem Chemicals, and the ligands $^iPr_2$Ph-DAB and *tert*-butyl isocyanide ($CNBu^t$) from Sigma-Aldrich, and used without further purification. NMR spectra were recorded on either a Varian INOVA 500 or a Bruker Advance II 400 spectrometer. ^{1}H, ^{19}F, and ^{13}C NMR spectra were referenced to residual solvent resonances. Infrared spectra were obtained on a Bruker Tensor 27 or Vertex 80 FTIR spectrometer. UV−vis spectra were obtained using a Perkin-Elmer Lambda 950 spectrometer. Mass spectral analysis for all compounds was performed by the laboratory for Biological Mass Spectroscopy at Texas A&M University, College Station, TX.

***fac*-Mn(Br)(CO)$_3$(^{i}Pr$_2$Ph-DAB) (1).** A round-bottom flask was charged with 0.318 g of $Mn(CO)_5Br$ (1.16 mmol), 0.436 g of $^iPr_2$Ph-DAB, and 20 mL of anhydrous diethyl ether under a nitrogen atmosphere. The solution was left overnight with constant stirring at room temperature. The solvent was evaporated to yield a solid violet colored residue which was redissolved in dichloromethane and upon evaporation of the solvent at 0 °C afforded 0.600 g (87% yield) of dark violet crystals of **1**. IR data in dichloromethane (ν_{CO} in cm^{-1}): 2035 (s), 1971 (s), 1930 (m). NMR data in $CDCl_3$: 1H δ 8.16 (s, 2 H), 7.17 (m, 6 H), 3.85 (s, 2 H), 2.69 (s, 2 H), 1.17 (s, 12 H), 1.92 (s, 12 H); ^{13}C{^{1}H} δ 164.5(s), 149.1(s), 140.4 (d), 128.5 (s, 1), 124.9 (t), 28.5(d), 26.9 (d), 23.3 (d). UV−vis data in dichloromethane (λ_{max}, nm): 366, 582. HRMS (EI$^+$) ; [M - Br]$^+$ (calc.), 515.210; [M - Br]$^+$ (exp.), 515.210.

***fac*-Mn(Br)(CO)$_3$(bpy) (bpy = 2,2′-bipyridine).** This complex was synthesized according to literature procedure[13] and characterized using IR spectroscopy in dichloromethane (ν_{CO} in cm^{-1}): 2022 (s), 1934 (s), 1912 (m).

[Mn(CO)$_4$(^{i}Pr$_2$Ph-DAB)]PF$_6$ (2). Method 1: A round-bottom flask was charged with 0.100 g of **1** (0.17 mmol), 0.075 g of $TlPF_6$ (0.21 mmol), and 20 mL of anhydrous dichloromethane under a nitrogen atmosphere. The solution was left overnight with constant stirring at room temperature. The reaction mixture was filtered through a Celite pad to remove thallium bromide and the filtrate was evaporated to yield a yellow oily residue which was washed several times with diethyl ether and dried in vacuo to afford 0.055 g (47% yield) of a yellow-orange solid, **2**. IR data in dichloromethane (ν_{CO} in cm^{-1}): 2109 (w), 2042 (sh), 2027 (s), 2006 (m). NMR data in $CDCl_3$: 1H δ 8.67 (s, 2 H), 7.47 (m, 6 H), 3.76 (s, 2 H), 2.83 (s, 2 H), 1.31 (s, 12 H); ^{19}F δ −72.1 (d, J = 712 Hz); ^{31}P δ −144.8 (septet, J = 712 Hz). UV−vis data in dichloromethane (λ_{max} in nm): 350, 406. HRMS (EI$^+$) [M - PF_6]$^+$ (calc.), 543.202; [M -PF_6]$^+$(exp.), 543.205. Method 2: A round-bottom flask was charged with 0.100 g of **1** (0.17 mmol), 0.065 g $TlPF_6$ (0.18 mmol), and 20 mL of anhydrous 1,2-dichlorethane under a nitrogen atmosphere. After stirring for 1 h at room temperature, CO gas was bubbled through the solution for 2 h. After additional stirring for 16 h, the solution was filtered through a Celite pad to remove thallium bromide and evaporated to yield a brown solid residue which was washed several times with diethyl ether and dried in vacuo to afford 0.088 g (75% yield) of yellow-orange solid, **2**.

***fac*-[Mn(CO)$_3$(^{i}Pr$_2$Ph-DAB)(CH$_3$CN)]PF$_6$ (3a).** A round-bottom flask was charged with 0.100 g of **1** (0.17 mmol), 0.087 g $TlPF_6$ (0.24 mmol), and 20 mL of anhydrous acetonitrile under nitrogen atmosphere. The solution was left overnight with constant stirring at room temperature. The reaction mixture was filtered through a Celite pad to remove thallium bromide and evaporated to yield a red residue which was washed several times with diethyl ether and dried in vacuo to afford 0.085 g (73% yield) of red solid, **3a**. IR data in dichloromethane (ν_{CO} in cm^{-1}): 2054 (s), 1979 (s), 1963 (m). NMR data in $CDCl_3$: 1H δ 8.50 (s, 2 H), 7.40 (m, 6 H), 3.10 (s, 2 H), 2.77 (s, 2 H), 2.54 (s, CH_3, acetonitrile), 1.28 (s, 12 H), 1.19 (s, 12 H); ^{19}F δ −73.3 (d, J = 712 Hz); ^{31}P δ −144.5 (pentet, J = 712 Hz). UV−vis data in dichloromethane (λ_{max} in nm): 365, 487. HRMS (EI$^+$) [M - PF_6]$^+$ (calc.), 556.232; [M - PF_6]$^+$ (exp.), 556.237.

***fac*-[Mn(CO)$_3$(^{i}Pr$_2$Ph-DAB)(CNBu^t)]PF$_6$ (3b).** A round-bottom flask was charged with 0.100 g of **1** (0.17 mmol), 0.070 g $TlPF_6$ (0.20 mmol), 0.022 g CN^tBu (0.26 mmol), and 20 mL of anhydrous dichloromethane under a nitrogen atmosphere. The solution was left overnight with constant stirring at room temperature. The reaction mixture was filtered through a Celite pad to remove thallium bromide, and the filtrate was evaporated to yield a red residue which was washed several times with hexane and dried in vacuo to afford 0.120 g (96% yield) of red solid, **3b**. IR data in dichloromethane (ν_{CO} in cm^{-1}): 2051 (s), 1983 (m, br), ν_{CN}: 2187 cm^{-1}. NMR data in $CDCl_3$: 1H δ 8.51 (s, 2 H), 7.40 (m, 6 H), 3.26 (s, 2 H), 2.58 (s, 2 H), 1.75 (s, Bu^t, 9 H), 1.42 (s, 12 H), 1.21 (s, 12 H); ^{19}F δ −72.3 (d, J = 734 Hz); ^{31}P δ −144.5 (pentet, J = 712 Hz). UV−vis data in dichloromethane (λ_{max} in nm): 356, 473. HRMS (EI$^+$) [M - PF_6]$^+$ (calc.), 598.257; [M - PF_6]$^+$ (exp.), 598.284.

***fac*-ReBr(CO)$_3$(^{i}Pr$_2$Ph-DAB) (4).** A round-bottom flask was charged with 0.220 g of $Re(CO)_5Br$ (0.54 mmol), 0.205 g $^iPr_2$Ph-DAB (0.54 mmol), and 20 mL of anhydrous toluene under a nitrogen atmosphere. The solution was refluxed with constant stirring for 3 h. After cooling to room temperature and evaporation of solvent, a solid purple colored residue was recovered which was redissolved in dichloromethane and upon slow evaporation of solvent at 0 °C afforded 0.340 g (86% yield) of dark violet crystals of **4**. IR data in dichloromethane (ν_{CO} in cm^{-1}): 2035 (s), 1971 (s), 1930 (m). NMR data in $CDCl_3$: 1H δ 8.68 (s, 2 H), 7.40 (m, 6 H), 4.00 (septet, 2 H), 2.77 (septet, 2 H), 1.36 (quartet, 12 H), 1.14 (quartet, 12 H); ^{13}C{^{1}H} δ 166.5 (s), 148.1 (s), 141.4 (d), 128.5 (s, 1), 124.9 (t), 28.5 (d), 26.9 (d), 23.0 (d). UV−vis data in acetonitrile (λ_{max}, nm): 325, 375, 499. HRMS (EI$^+$) ; [M - Br]$^+$ (calc.), 647.223; [M - Br]$^+$ (exp.), 647.228.

CW Photolysis Experiments (CO release studies). The light source for these experiments was a 100 W Xe arc lamp coupled to a monochromator to isolate the appropriate photolysis wavelength. The irradiation power at the sample was measured to be 0.3 mW with an optical power meter (ThorLabs). The samples were prepared in dim light and placed in an IR cell with CaF_2 windows positioned 2 cm away from the exit slit of the monochromator. The changes in the IR spectra during irradiation were monitored with a Bruker Vertex 80 FTIR.

Time Resolved IR Studies. Samples were irradiated in a 0.75 mm path length temperature controlled cell (Harrick Scientific) with CaF_2 windows using 355 nm light from a Nd:YAG laser (Quantel, Brilliant B). For low temperature experiments, a 0.5 mm path length variable temperature IR cell (Specac) was used. Changes in the IR spectra following a single shot of the UV laser were monitored using rapid scan FTIR (Bruker Vertex 80).

X-ray Crystallography. Diffraction data for **1**, **2**, **3a**, **3b**, and **4** were obtained by placing the crystals under streaming nitrogen (150 K) in a SMART Apex CCD diffractometer. The space groups were determined on the basis of systematic absences and intensity statistics. The structures were solved by direct methods and refined by full-matrix least-squares on F^2. Anisotropic displacement parameters were determined for all non-hydrogen atoms. Hydrogen atoms were placed at idealized positions and refined with fixed isotropic displacement parameters. The following is a list of programs used: data collection and cell refinement, APEX2;[14] data reductions, SAINTPLUS version 6.63;[15] absorption correction, SADABS;[16] structural solutions, SHELXS-97;[17] structural refinement, SHELXL-97;[18] graphics and

dx.doi.org/10.1021/ic500025k | Inorg. Chem. 2014, 53, 4081−4088

publication materials, Mercury version 3.0.[19] The data is available in the Supporting Information.

DFT Calculations. All calculations were performed in the Gaussian 09 suite of programs using density functional theory (DFT).[20] All geometries were optimized with the ωB97XD functional[21] using the Def2-SVP basis set.[22] Frequency calculations were also performed on the optimized geometries to confirm energy minima by the absence of imaginary frequencies.

RESULTS AND DISCUSSION

$MnBr(CO)_3(^iPr_2Ph\text{-}DAB)$ (1). Reaction of $Mn(CO)_5Br$ with the $^iPr_2Ph$-DAB ligand at room temperature affords **1** in good yield. The crystal structure (Figure 2) shows a facial

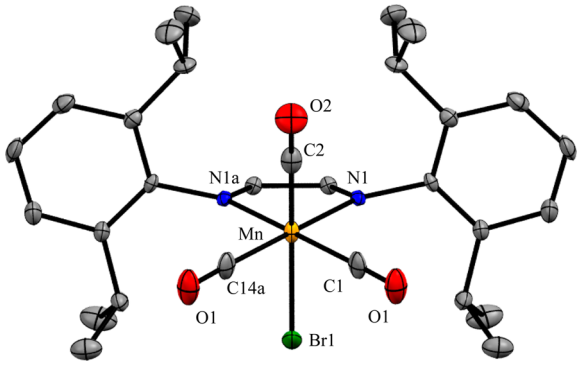

Figure 2. Thermal ellipsoid (probability level 50%) plot of **1** with select atom labeling. Hydrogen atoms omitted for clarity.

arrangement of the CO ligands and the relative intensities of the three CO stretching bands observed in the IR spectrum (Table 1) are consistent with this geometry. An interesting structural feature in **1** is the significant deviation from linearity in the axial ∠Br−Mn−CO = 172.51°, which is most likely due to steric congestion around the Mn center because of the bulky $^iPr_2Ph$-DAB ligand. This bond angle is in good agreement with a DFT calculated value of 170.71° and indicates the level of theory applied is suitable for describing the current systems. The extent of this angular deviation is unusual by comparison with other $Mn(Br)(CO)_3$(diimine) complexes in which the axial ∠CO−Mn−Br ranges from 177.54° to 178.89°.[11e,23] In the electronically similar yet sterically different $Mn(Br)(CO)_3$(Ph-DAB) complex, DFT calculations predict an almost linear (179.9°) ∠CO−Mn−Br.

The Re analog (**4**) was also synthesized and compared to **1**; the crystal structure (Figure S1) indicates a larger value for the axial ∠CO−Re−Br = 176.05°. The steric influence of the $^iPrPh_2$-DAB ligand upon this bond angle is diminished in this case as the larger Re center provides more space to accommodate the coordinated ligands. To isolate the steric impact upon the Mn−CO interaction in this complex, the Mn−CO bond dissociation enthalpy (BDE) in **1** and in the less encumbered *fac*-$Mn(Br)(CO)_3$(Ph-DAB) species was calculated using DFT. The Mn−CO BDEs calculated at 37.1 kcal/mol (axial) and 26.9 kcal/mol (equatorial) were found to be significantly lower in **1** compared to *fac*-$Mn(Br)(CO)_3$(Ph-DAB) at 49.6 kcal/mol (axial) and 34.1 kcal/mol (equatorial). The weakening of the Mn−CO bond as a result of increased steric crowding around the metal center suggests that the $^iPr_2Ph$-DAB ligand may be of utility in the design of efficient CORMs or photoCORMs.

Visible Light Photolysis. When a heptane solution of **1** is exposed to room light at ambient temperature, the color changes from dark violet to yellow within 30 min. This reaction is reversible and, in the absence of light, the yellow solution converts back to dark violet. IR analysis of the yellow solution indicates the presence of $Mn(CO)_5Br$ and evaporation resulted in the isolation of yellow crystals which were confirmed to be the free $^iPr_2Ph$-DAB ligand by X-ray analysis. The reversibility in the dark can then be explained as a thermal reaction between the free diimine ligand and the pentacarbonyl to reform **1**. Complex **1** is stable in the dark for several days without decomposition. Due to biological considerations, an important design parameter for photoCORMs is the requirement that they release CO upon visible light irradiation. The wavelength range for such photodynamic therapies is generally 630−850 nm, and viable targets should undergo CO release under these irradiation conditions.[24] While most photoCORMs readily demonstrate CO release under UV irradiation,[11d,e,h,25] very few examples exist for similar photo activity with visible light (λ > 400 nm). Complex **1** has an absorption maxima at 582 nm (CH_2Cl_2), and to determine the rate of CO photorelease, its decomposition was monitored by IR spectroscopy following irradiation at 560 nm. As shown in Figure 3, the CO bands of **1** steadily decrease in intensity without the formation of any intermediates that could be detected under these conditions. A small broad peak at 2140 cm^{-1} grows in and is assigned to free CO in solution providing clear evidence for CO release upon visible light photolysis. The half-life for the CO release process was 12 min and, given the low power of the light source used (0.3 mW), this rate compares very favorably to those found for some other Mn complexes. For example, photolysis of $[Mn(CO)_3(tpa)]ClO_4$ (tpa = tris(2-pyridyl)amine) with ∼100 mW visible light (λ > 350 nm) yields an apparent CO release rate constant of 6×10^{-3} s^{-1} ($t_{1/2}$ = 2 min).[11g]

Recently, rapid CO photorelease from two manganese complexes at λ > 520 nm was reported.[26] Thus, complex **1**, which exhibits CO dissociation at 560 nm, is a rare example of a visible light induced photoCORM.[11f,l] While more rigorous experiments, to include myoglobin assays and quantification of

Table 1. CO Stretching Wavenumbers for Several Complexes at 293 K[a]

complex	ν_{CO} (cm^{-1}) (exp)	ν_{CO} (cm^{-1}) (calc.)[c]
$Mn(Br)(CO)_3$(R-DAB) (**1**)	2035, 1971, 1930	2189, 2142, 2093
$Mn(Br)(CO)_3$(bpy)	2022, 1934, 1912	
$[Mn(CO)_4$(R-DAB)$][PF_6]$ (**2**)	2109, 2042, 2027, 2006	2253, 2197, 2187, 2181
$[Mn(CH_3CN)(CO)_3$(R-DAB)$][PF_6]$ (**3a**)	2054, 1979, 1963	2215, 2162, 2145
$[Mn(THF)(CO)_3$(R-DAB)$][PF_6]$	2055, 1979, 1965	2206, 2142, 2135
$[Mn(DHF)(CO)_3$(R-DAB)$][PF_6]$	2053, 1979, 1964	
$[Mn(CN^tBu)(CO)_3$(R-DAB)$][PF_6]$ (**3b**)	2187 (CN), 2051, 1983[b]	2211, 2161, 2159

[a][R = $^iPr_2Ph$, bpy = bipyridyl]. Unless otherwise noted, solvent = CH_2Cl_2. [b]Broad. [c]Unscaled.

dx.doi.org/10.1021/ic500025k | Inorg. Chem. 2014, 53, 4081−4088

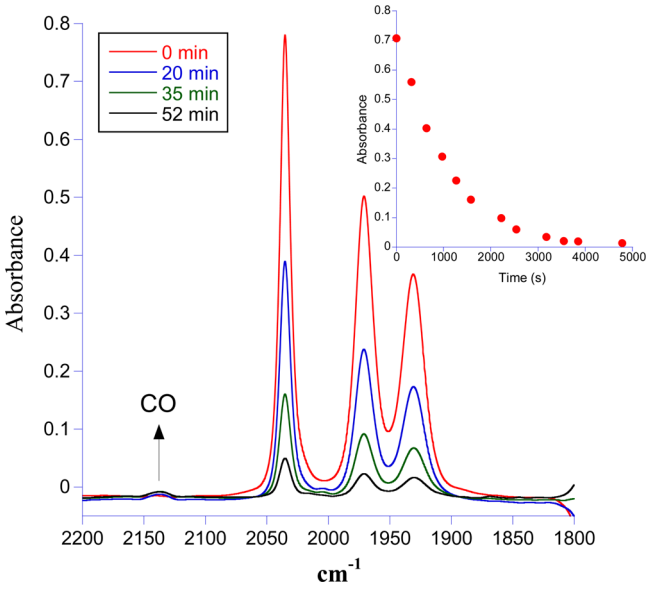

Figure 3. IR spectra obtained upon exposure of **1** to 560 nm light. Inset shows the decay of the 2035 cm^{-1} peak as a function of time.

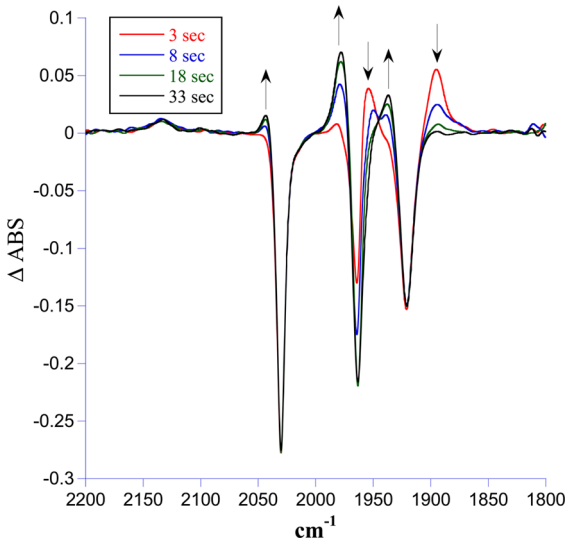

Figure 4. Spectral changes upon 355 nm photolysis of a THF solution of **1** at 228 K. The initially formed Mn(Br)(THF)$(CO)_2$(^{i}Pr_2Ph-DAB) species (1952 cm^{-1}, 1895 cm^{-1}) converts to the *mer*-Mn(Br)-$(CO)_3$(^{i}Pr_2Ph-DAB) isomer (2043 cm^{-1}, 1978 cm^{-1}, 1936 cm^{-1}) within 33 s of photolysis.

CO release, are required to assess the feasibility of such complexes for their use as photoCORMs, our intent was simply to demonstrate the unusual dissociation of the Mn−CO bond in **1** under visible light irradiation. By analogy with similar diimine complexes, visible light induced cleavage of the Mn−CO bond is likely due to a MLCT transition from a combination Mn(1)−CO π and Br p centered orbital to the π^* orbitals of the diimine ligand resulting in reduced Mn → CO π backbonding and subsequent CO loss.[11f,26] To provide support for this explanation, Tamm-Dancoff time dependent density functional calculations were performed on complex **1**. A calculated transition at 563 nm has a major contribution from the promotion HOMO-1 → LUMO which were found to have orbital characteristics (Figures S3, S4) similar to the other diimine systems mentioned above.

UV Photolysis. Previous studies have demonstrated that Mn(Br)$(CO)_3$(R-DAB) complexes (R = ^{i}Pr_2, t-Bu) undergo *fac* → *mer* isomerization upon UV photolysis.[9] Ultrafast studies show that the isomerization proceeds by way of equatorial CO dissociation (<400 fs) followed by Br movement (11 ps) from the axial to equatorial plane and reattachment of CO to yield the meridonal species.[27] To study the effect of the ^{i}Pr_2Ph-DAB ligand upon the rate of this isomerization, a THF solution of **1** was photolyzed with 355 nm light from a Nd:YAG laser. At 228 K, the spectral changes shown in Figure 4 confirm the initial formation of a dicarbonyl complex absorbing at 1952 cm^{-1} and 1895 cm^{-1} which converts to a species with three CO bands. By analogy with previous studies,[9h] the dicarbonyl species is assigned to the solvated Mn(Br)(THF)$(CO)_2$(^{i}Pr_2Ph-DAB) complex, and based on the relative intensities of the three CO bands, the final product is identified as the meridonal isomer (Scheme 1). A similar experiment was conducted with the less sterically encumbered Mn(Br)$(CO)_3$(bpy) complex. At 228 K, the rate of conversion from the THF solvate to the meridonal isomer was 20 times faster for complex **1** compared to Mn(Br)$(CO)_3$(bpy). The difference in rates may be attributed to differences in the steric profile of the bpy and ^{i}Pr_2Ph-DAB ligands and the resulting impact upon the Mn-THF bond strength. DFT calculations are consistent with this conclusion

Scheme 1

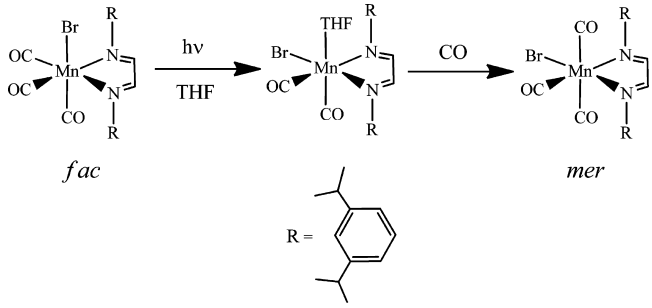

and show that the Mn-THF bond in Mn(Br)(THF)-$(CO)_2$(^{i}Pr_2Ph-DAB) (14.7 kcal/mol) is almost 10 kcal/mol weaker than in Mn(Br)$(CO)_3$(bpy) (24.5 kcal/mol). However, the transition state for the final step in the isomerization is not likely to involve significant Mn−THF bond disruption, since a 10 kcal/mol difference in BDE would result in a larger difference in rate than that observed here.

The results presented above suggest that the ^{i}Pr_2Ph-DAB ligand imparts unusual structural and photoreactivity properties to complex **1**, primarily as a result of the steric bulk of this molecule. To assess the influence of this ligand upon the thermal reactivity of the Mn−CO bond in a molecule with a higher CO to metal ratio, an important design consideration in CORMs, the ionic complex, [Mn$(CO)_4$(^{i}Pr_2Ph-DAB)][PF_6] (**2**), was synthesized.

[Mn$(CO)_4$(^{i}Pr_2Ph-DAB)][PF_6](2). Addition of $TlPF_6$ to a dichloromethane solution of **1** in the absence of added CO followed by crystallization provided **2** in low yield. As shown in Scheme 2, initial generation of the Lewis acid−base adduct [Mn$(CO)_3$(^{i}Pr_2Ph-DAB)(PF_6)] followed by its partial decomposition during the crystallization process to generate CO which can coordinate to the residual tricarbonyl likely results in the formation of **2**.[28] When the reaction was conducted in the presence of added CO a much improved yield of **2** was realized. The crystal structure of **2** is shown in Figure 5. As expected of a

dx.doi.org/10.1021/ic500025k | *Inorg. Chem.* 2014, 53, 4081−4088

Scheme 2

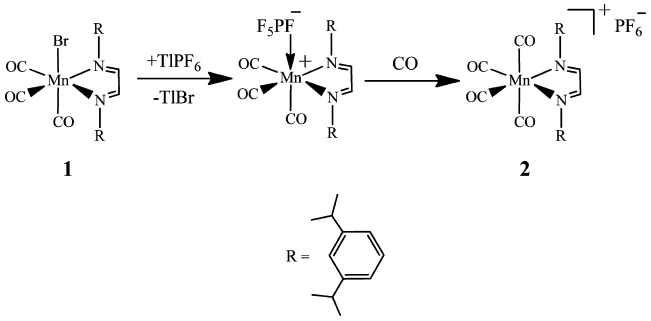

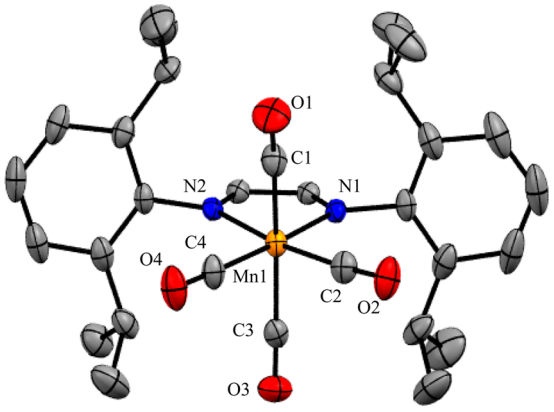

Figure 5. Thermal ellipsoid (probability level 50%) plot of **2** with select atom labeling. Hydrogen atoms and counteranion omitted for clarity.

cationic complex with four strong π accepting ligands, the CO stretching bands in **2** are shifted to significantly higher wavenumbers relative to **1** (Table 1). Similar to **1**, the steric influence of the $^{i}P_2$Ph-DAB ligand upon the geometry of **2** is evident in the axial ∠CO−Mn−CO, which at 170.75° is significantly less than that found in analogous complexes where this angle ranges from 174.14° to 178.9°.[29]

Thermal Reactivity. The expected weakening of the Mn−CO bonds due to the crowded metal center in **2** is strikingly apparent in the thermal reactivity of this complex. For example, dissolution of the yellow-orange solid in acetonitrile at 288 K results in an instantaneous color change to red. The IR spectrum of this red solution shows three peaks with relative intensities suggestive of a facial tricarbonyl complex. This species was isolated and the crystal structure shown in Figure 6 confirms its identity as the acetonitrile complex [Mn(CH_3CN)-$(CO)_3$($^{i}Pr_2$Ph-DAB)][PF_6] (**3a**).

To monitor the formation of the acetonitrile adduct, a dichloromethane solution of **2** was reacted with 0.5 M CH_3CN at 288 K. The IR spectral changes shown in Figure 7 confirm a clean conversion of **2** into **3a** under these conditions. Unfortunately, the mechanism of this substitution reaction and the possibility of estimating the Mn−CO bond enthalpy could not be investigated, because at higher temperatures and concentrations of CH_3CN, additional unassigned peaks were observed and the rate of decay of **2** did not match the growth of the product. An associative mechanism for CO substitution appears unlikely given the steric bulk of the $^{i}Pr_2$Ph-DAB ligand. However, when the concentration of CO was increased by bubbling it through the reaction solution for several minutes, no significant effect (less than a factor of 2) was observed on

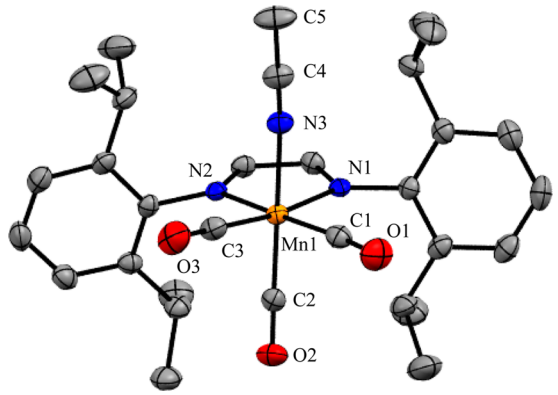

Figure 6. Thermal ellipsoid (probability level 50%) plot of **3a** with select atom labeling. Hydrogen atoms and counteranion omitted for clarity.

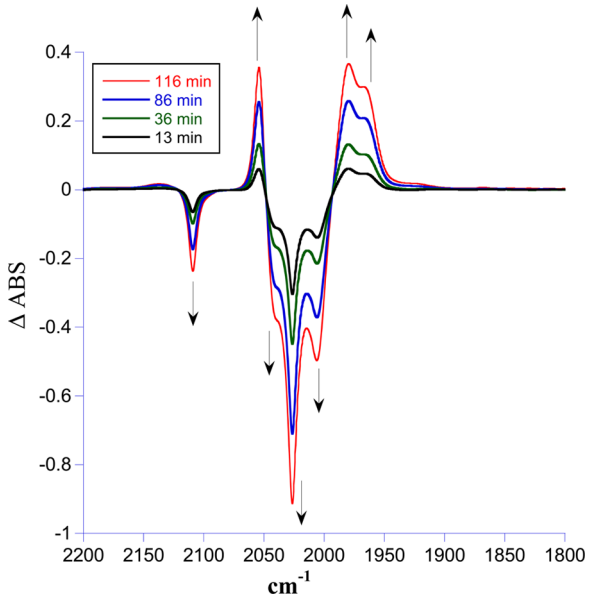

Figure 7. Spectral changes observed upon reaction of a dichloromethane solution of **2** with 0.5 M CH_3CN at 288 K to yield **3a**.

the decay rate of **2**. This observation is not consistent with a dissociative substitution mechanism either and would suggest an interchange (I_a or I_d) pathway for the displacement of CO from **2**.

Spectral changes in the infrared observed upon dissolution of **2** in other coordinating solvents such as THF and 2,3-dihydrofuran (DHF) suggest the displacement of an axial CO ligand at room temperature to form the [Mn(THF)-$(CO)_3$($^{i}Pr_2$Ph-DAB)][PF_6] and [Mn(DHF)$(CO)_3$($^{i}Pr_2$Ph-DAB)][PF_6] complexes, respectively. The rate of CO substitution is slower in these solvents compared to CH_3CN. More basic ligands such as pyridine and other amines reacted with **2** to afford a monocarbonyl complex (single peak in the IR spectrum) which was unstable and could not be isolated.

Despite the different donor characteristics of the solvent ligands, the substituted tricarbonyl complexes have similar CO stretching wavenumbers (Table 1). This observation suggests that the electronic environment of the Mn center is not influenced by the ligand donor/acceptor abilities. To ascertain the extent of this insensitivity, the isonitrile ligand CNt-Bu, with electronic characteristics significantly different than those of

dx.doi.org/10.1021/ic500025k | *Inorg. Chem.* 2014, 53, 4081−4088

THF and CH_3CN, was used to synthesize the [Mn(CNt-Bu)$(CO)_3$(iPr_2Ph-DAB)][PF_6] (**3b**) complex. The crystal structure of **3b** is shown in Figure 8.

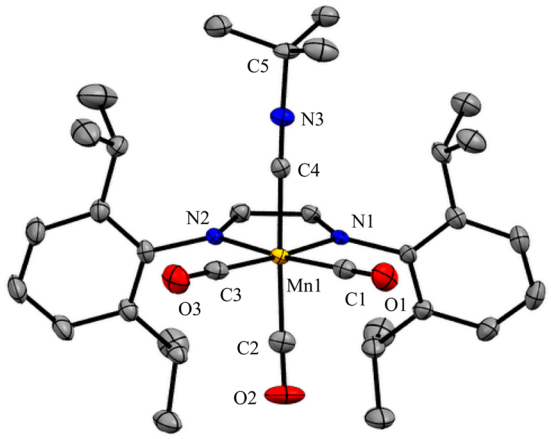

Figure 8. Thermal ellipsoid (probability level 50%) plot of **4b** with select atom labeling. Hydrogen atoms and counteranion omitted for clarity. The unit cell contains two identical molecules.

Similar to the structures observed for **1**, **2**, and **3a**, the axial ∠CO−Mn−CNt−Bu = 172.38° shows a large deviation from linearity. Surprisingly, the CO stretching wavenumbers in this species are comparable to those of the other solvated complexes (Table 1). Since DAB ligands are considered to be electron reservoirs,[30] it is possible that they impart a "leveling" effect upon the metal electron density resulting in similar CO stretching wavenumbers for several of the observed complexes. The DFT calculated CO band positions for these complexes (Table 1) are also within 20 cm^{-1} (unscaled) of each other. The extreme lability of the CO ligand in **2** is in dramatic contrast to similar complexes such as $[Mn(CO)_4(phen)]^+$ and $[Mn(CO)_4(dppe)]^+$ which demonstrate CO substitution only at high temperatures.[31] For example, $[Mn(CO)_4(dppe)]^+$ is stable for several months in acetonitrile at room temperature.

As shown in Table 2, the Mn−CO bond in **2** is remarkably weak (BDE = 25.3 kcal/mol) especially compared to that in

Table 2. Calculated Mn−L BDEs for Several Complexes Demonstrating the Steric Influence of the Diimine Ligand upon the Strength of This Interaction

L	$[Mn(L)(CO)_3(^iPr_2Ph\text{-}DAB)]^+$ (kcal/mol)	$[Mn(L)(CO)_3(Ph\text{-}DAB)]^+$ (kcal/mol)
CO	25.3	35.4
CH_3CN	30.1	40.3
THF	26.1	41.6
CNtBu	43.5	52.8

$[Mn(CO)_4(Ph\text{-}DAB)]^+$ (35.4 kcal/mol) and $[Mn(CO)_4(bpy)]^+$ (31.4 kcal/mol). Given the similar Mn−CO BDEs in these latter two complexes, the weaker interaction in **2** is clearly a result of steric rather than electronic differences between the diimine ligands. In a related Mn complex, (η^3-allyl)$Mn(CO)_4$, increasing the steric bulk of the allyl ligand also resulted in an increase in the rate of CO loss.[32] Since facile loss of coordinated CO ligands is an important characteristic of CORMs, these findings suggest that incorporation of the bulky $^iPr_2$Ph-DAB ligand into metal carbonyl complexes may be useful in the synthesis of viable targets.

In agreement with experimental findings, the DFT calculations predict that displacement of CO in **2** by CH_3CN and THF is thermodynamically favored with $\Delta G°_{rxn}$ (298 K) = −5.7 kcal/mol and −1.5 kcal/mol, respectively. In all cases, Mn−L BDEs are calculated to be significantly lower in complexes with the larger ($^iPr_2$Ph-DAB) ligand compared to those of the electronically similar yet smaller (Ph-DAB) ligand. Of all the ionic complexes studied, calculations indicate that the strongest interaction is between the Mn center and the isonitrile ligand. This observation is consistent with the greater σ donating ability of isonitrile compared to the other ligands used and, as expected for a cationic complex, suggests a reduced role for π backbonding in stabilizing the Mn-L interaction.

Photoactivity. Compared to **1**, complex **2** shows enhanced thermal reactivity with respect to CO loss. However, unlike **1**, it is stable in room light. For example, a dichloromethane solution of **2** showed no evidence of decomposition after several hours under room light. This relative photostability is also manifested in the rate of CO release from **2** compared to **1**. While irradiation of **2** at its absorption maxima of 420 nm results in CO release, the half-life of 180 min is significantly longer than that observed for **1** (35 min) under similar conditions.

CONCLUSIONS

The coordination of a bulky diimine ligand, $^iPr_2$Ph-DAB, to a Mn(1) center yields complexes with unusual thermal and photochemical properties that may be of utility in the design of CORMs or photoCORMs. For example, while UV photolysis of metal carbonyl complexes results in CO loss, *fac*-Mn(Br)-$(CO)_3(^iPr_2Ph\text{-}DAB)$ demonstrates facile photochemical CO release under visible light (560 nm) irradiation. In contrast to some cationic manganese tetracarbonyl complexes which are stable toward thermal displacement of CO, the cationic complex $[Mn(CO)_4(^iPr_2Ph\text{-}DAB)][PF_6]$ undergoes rapid substitution of CO, even by solvent molecules such as CH_3CN and THF. Thus, dissolution of the tetracarbonyl complex in acetonitrile at 288 K results in instantaneous formation of *fac*-$[Mn(CH_3CN)(CO)_3(^iPr_2Ph\text{-}DAB)][PF_6]$ species. The crystal structures of the synthesized complexes are consistent with considerable crowding around the metal center and theoretical calculations using DFT confirm the weakening of the metal−CO interaction is primarily due to the steric bulk of the diimine ligand. These results indicate the possible use of the $^iPr_2$Ph-DAB ligand in the synthesis of reactive metal carbonyl complexes with applications as CORMs or other photoactive materials.

ASSOCIATED CONTENT

Supporting Information

X-ray crystallographic data for **1**, **2**, **3a**, **3b**, and **4**. UV−vis spectra and calculated structures for the modeled complexes. This material is available free of charge via the Internet at http://pubs.acs.org.

AUTHOR INFORMATION

Corresponding Authors

*E-mail: djdarens@mail.chem.tamu.edu (D.J.D.).
*E-mail: ashfaq.bengali@qatar.tamu.edu (A.A.B).

Notes

The authors declare no competing financial interest.

■ ACKNOWLEDGMENTS

This publication was made possible by funding from the Qatar National Research Fund (member of Qatar Foundation). The experimental work was supported by NPRP grant 4-1517-1-245 and the theoretical studies by NPRP grant 09-143-1-022. The statements made herein are solely the responsibility of the authors.

■ REFERENCES

(1) (a) Baker, R. J.; Jones, C.; Mills, D. P.; Pierce, G. A.; Waugh, M. *Inorg. Chim. Acta* **2008**, *361*, 427−435. (b) Dong, Q.; Su, J.-H.; Gong, S.; Li, Q.-S.; Zhao, Y.; Wu, B.; Yang, X.-J. *Organometallics* **2013**, *32*, 2866−2869. (c) Dong, Q.; Zhao, Y.; Su, Y.; Su, J.-H.; Wu, B.; Yang, X.-J. *Inorg. Chem.* **2012**, *51*, 13162−13170. (d) Gao, J.; Li, S.; Zhao, Y.; Wu, B.; Yang, X.-J. *Organometallics* **2012**, *31*, 2978−2985. (e) Greulich, S.; Kaim, W.; Stange, A. F.; Stoll, H.; Fiedler, J.; Záliš, S. *Inorg. Chem.* **1996**, *35*, 3998−4002. (f) Koten, G. V.; Vrieze, K. *Adv. Organomet. Chem.* **1982**, *21*, 151−239. (g) Ray, K.; Petrenko, T.; Wieghardt, K.; Neese, F. *Dalton Trans.* **2007**, *35*, 1552−1566.

(2) (a) Kumar, A.; Sun, S.-S.; Lees, A. *Top. Organomet Chem.* **2010**, *29*, 37−71. (b) Nieuwenhuis, H. A.; Stufkens, D. J.; Oskam, A. *Inorg. Chem.* **1994**, *33*, 3212−3217. (c) Vlček, A., Jr. *Photophysics of Organometallics* **2010**, *29*, 115−158.

(3) (a) Bock, H.; tom Dieck, H. *Angew. Chem., Int. Ed.* **1966**, *5*, 520−522. (b) Vrieze, K. *J. Organomet. Chem.* **1986**, *300*, 307−326.

(4) (a) Bigioni, M.; Ganis, P.; Panunzi, A.; Ruffo, F.; Salvatore, C.; Vito, A. *Eur. J. Inorg. Chem.* **2000**, *2000*, 1717−1721. (b) Ferrara, M. L.; Giordano, F.; Orabona, I.; Panunzi, A.; Ruffo, F. *Eur. J. Inorg. Chem.* **1999**, *1999*, 1939−1947. (c) Togni, A.; Venanzi, L. M. *Angew. Chem., Int. Ed.* **1994**, *33*, 497−526. (d) Vrieze, K. *J. Organomet. Chem.* **1986**, *300*, 307−326.

(5) (a) Burgess, J.; Chambers, J.; Haines, R. *Trans. Met. Chem.* **1981**, *6*, 145−151. (b) Guillon, T.; Boggio-Pasqua, M.; Alary, F.; Heully, J.-L.; Lebon, E.; Sutra, P.; Igau, A. *Inorg. Chem.* **2010**, *49*, 8862−8872. (c) Kalyanasundaram, K. *Coord. Chem. Rev.* **1982**, *46*, 159−244. (d) Piau, R. E.; Guillon, T.; Lebon, E.; Perrot, N.; Alary, F.; Boggio-Pasqua, M.; Heully, J.-L.; Juris, A.; Sutra, P.; Igau, A. *New. J. Chem.* **2012**, *36*, 2484−2492. (e) Záliš, S.; Ben Amor, N.; Daniel, C. *Inorg. Chem.* **2004**, *43*, 7978−7985.

(6) (a) Guan, Z.; Popeney, C. *Top. Cat.* **2009**, *26*, 179−220. (b) Ittel, S. D.; Johnson, L. K.; Brookhart, M. *Chem. Rev.* **2000**, *100*, 1169−1204. (c) Yuan, J.; Wang, X.; Mei, T.; Liu, Y.; Miao, C.; Xie, X. *Trans. Met. Chem.* **2011**, *36*, 433−439.

(7) (a) Hartl, F.; Aarnts, M. P; Peelen, K. *Collect. Czech. Chem. Commun.* **1996**, *61*, 1342−1352. (b) Johnson, F. P. A.; George, M. W.; Hartl, F.; Turner, J. J. *Organometallics* **1996**, *15*, 3374−3387. (c) Rossenaar, B. D.; Hartl, F.; Stufkens, D. J. *Inorg. Chem.* **1996**, *35*, 6194−6203. (d) Kumar, B.; Llorente, M.; Froehlich, J.; Dang, T.; Sathrum, A.; Kubiak, C. P. *Annu. Rev. Phys. Chem.* **2012**, *63*, 541−569. (e) Rossenar, B. D.; Hartl, F.; Stufkens, D. J. *Inorg. Chem.* **1996**, *35*, 6194−6203.

(8) (a) Chartrand, D.; Castro Ruiz, C. A.; Hanan, G. S. *Inorg. Chem.* **2012**, *51*, 12738−12747. (b) Sacksteder, L.; Lee, M.; Demas, J. N.; DeGraff, B. A. *J. Am. Chem. Soc.* **1993**, *115*, 8230−8238. (c) Sacksteder, L.; Zipp, A. P.; Brown, E. A.; Streich, J.; Demas, J. N.; DeGraff, B. A. *Inorg. Chem.* **1990**, *29*, 4335−4340. (d) Wrighton, M.; Morse, D. L. *J. Am. Chem. Soc.* **1974**, *96*, 998−1003. (e) Li, Y.; Liu, Y.; Guo, J.; Wu, F.; Tian, W.; Li, B.; Wang, Y. *Synth. Met.* **2001**, *118*, 175.

(9) (a) Hartl, F.; Mahabiersing, T.; Le Floch, P.; Mathey, F.; Ricard, L.; Rosa, P.; Záliš, S. *Inorg. Chem.* **2003**, *42*, 4442−4455. (b) Hartl, F.; Rosa, P.; Ricard, L.; Le Floch, P.; Záliš, S. *Coord. Chem. Rev.* **2007**, *251*, 557−576. (c) Kleverlaan, C. J.; Hartl, F.; Stufkens, D. J. *J. Organomet. Chem.* **1998**, *561*, 57−65. (d) Kokkes, M. W.; Stufkens, D. J.; Oskam, A. *Inorg. Chem.* **1985**, *24*, 2934−2942. (e) Rosa, A.; Ricciardi, G.; Baerends, E. J.; Stufkens, D. J. *J. Phy. Chem.* **1996**, *100*, 15346−15357. (f) Rosa, A.; Ricciardi, G.; Baerends, E. J.; Stufkens, D. J. *Inorg. Chem.* **1998**, *37*, 6244−6254. (g) Stor, G. J.; Morrison, S. L.; Stufkens, D. J.; Oskam, A. *Organometallics* **1994**, *13*, 2641−2650. (h) Kleverlaan, C. J.; Hartl, F.; Stufkens, D. J. *J. Photochem. Photobiol. A* **1997**, *103*, 231.

(10) Chen, H.; Bartlett, R. A.; Dias, H. V. R.; Olmstead, M. M.; Power, P. P. *Inorg. Chem.* **1991**, *30*, 2487−2494. (b) García-Escudero, L. A.; Miguel, D.; Turiel, J. A. *J. Organomet. Chem.* **2006**, *691*, 3434−3444. (c) Ghosh, M.; Weyhermuller, T.; Wieghardt, K. *Dalton Trans.* **2008**, *37*, 5149−5151. (d) Graham, A. J.; Akrigg, D.; Sheldrick, B. *Cryst. Struct. Commun.* **1977**, *6*, 571.

(11) (a) Schatzschneider, U. *Eur. J. Chem.* **2010**, *10*, 1451−1467. (b) Motterlini, R.; Otterbein, L. E. *Nature* **2010**, *9*, 728−743. (c) Crook, S. H.; Mann, B. E.; Meijer, A. J. H. M.; Adams, H.; Sawle, P.; Scapens, D. A.; Motterlini, R. A. *Dalton Trans.* **2011**, *40*, 4230−4235. (d) Dordelmann, G.; Meinhardt, T.; Sowik, T.; Krueger, A.; Schatzschneider, U. *Chem. Commun.* **2012**, *48*, 11528−11530. (e) Dördelmann, G.; Pfeiffer, H.; Birkner, A.; Schatzschneider, U. *Inorg. Chem.* **2011**, *50*, 4362−4367. (f) Gonzalez, M. A.; Carrington, S. J.; Fry, N. L.; Martinez, J. L.; Mascharak, P. K. *Inorg. Chem.* **2012**, *51*, 11930−11940. (g) Gonzalez, M. A.; Yim, M. A.; Cheng, S.; Moyes, A.; Hobbs, A. J.; Mascharak, P. K. *Inorg. Chem.* **2011**, *51*, 601−608. (h) Govender, P.; Pai, S.; Schatzschneider, U.; Smith, G. S. *Inorg. Chem.* **2013**, *52*, 5470−5478. (i) Hallett, A. J.; Angharad Baber, R.; Guy Orpen, A.; Ward, B. D. *Dalton Trans.* **2011**, *40*, 9276−9283. (j) Pfeiffer, H.; Rojas, A.; Niesel, J.; Schatzschneider, U. *Dalton Trans.* **2009**, *38*, 4292−4298. (k) Rudolf, P.; Kanal, F.; Knorr, J.; Nagel, C.; Niesel, J.; Brixner, T.; Schatzschneider, U.; Nuernberger, P. *J. Phys. Chem. Lett.* **2013**, *4*, 596−602. (l) Ward, J. S.; Lynam, J. M.; Moir, J. W. B.; Sanin, D. E.; Mountford, A. P.; Fairlamb, I. J. S. *Dalton Trans.* **2012**, *41*, 10514−10517. (m) Mohr, F.; Niesel, J.; Schatzschneider, U.; Lehmann, C. W. *Z. Anorg. Allg. Chem.* **2012**, *638*, 543−546.

(12) (a) Eiβler, A.; Kläring, P.; Emmerling, F.; Braun, T. *Eur. J. Inorg. Chem.* **2013**, *2013*, 4775−4788. (b) Li, J.; Zhang, K.; Huang, H.; YU, A.; Hu, H.; Cui, H.; Cui, C. *Organometallics* **2013**, *32*, 1630−1635.

(13) Staal, L. H.; Oskam, A.; Vrieze, K. *J. Organomet. Chem.* **1979**, *170*, 235−245.

(14) *APEX2*, v 2009.7−0; Bruker AXS, Inc., Madison, WI, 2007.

(15) *SAINTPLUS: Program for Reduction of Area Detector Data*, 1034, v 6.63; Bruker AXS Inc., Madison, WI, 2007.

(16) Sheldrick, G. M., *SADABS: Program for Absorption Correction of 1036 Area Detector Frames*; Bruker AXS Inc., Madison, WI, 2001.

(17) Sheldrick, G. M., *SHELXS-97: Program for Crystal Structure 1038 Solution*; Universität Göttingen, Göttingen, Germany, 1997.

(18) Sheldrick, G. M., *SHELXL-97: Program for Crystal Structure 1040 Refinement*; Universität Göttingen, Göttingen, Germany, 1997.

(19) Macrae, C. F.; Edgington, P. R.; McCabe, P.; Pidcock, E.; Shields, G. P.; Taylor, R.; Towler, M.; van de Streek, J. *J. Appl. Crystallogr.* **2006**, *39*, 453−457.

(20) Frisch, M. J.; et al. *Gaussian 09*, revision B.01; Gaussian Inc., Wallingford, CT, 2009.

(21) Chai, J. D.; Head-Gordon, M. *Phys. Chem. Chem. Phys.* **2008**, *10*, 6615−6620.

(22) Weigend, F.; Ahlrichs, R. *Phys. Chem. Chem. Phys.* **2005**, *7*, 3297−3305.

(23) (a) García-Escudero, L. A.; Miguel, D.; Turiel, J. A. *J. Organomet. Chem.* **2006**, *691*, 3434−3444. (b) Valín, M. L.; Moreiras, D.; Solans, X.; Font-Altaba.; García-Alonso, F. J. *Acta Crystallogr., Sect. C* **1986**, *42*, 417−418. (c) Graham, A. J.; Akrigg, D.; Sheldrick, B. *Cryst. Struct. Commun.* **1977**, *6*, 571. (d) Alvarez, C. M.; Garcia-Rodriguez, R.; Miquel, D. *Dalton Trans.* **2007**, *36*, 3546−3554.

(24) (a) Szacilowski, K.; Macyk, W.; Drzewiecka-Matuszek, A.; Brindell, M.; Stochel, G. *Chem. Rev.* **2005**, *105*, 2647−2694. (b) Farrer, N. J.; Salassa, L.; Sadler, P. J. *Dalton Trans.* **2009**, *38*, 10690−10701.

(25) (a) Niesel, J.; Pinto, A.; N'DOngo, H. W. P.; Merz, K.; Ott, I.; Gust, R.; Schatszsschneider, U. *Chem. Commun.* **2008**, *44*, 1798−1800. (b) Kunz, P. C.; Huber, W.; Rojas, A.; Schatszsschneider, U.; Spingler, B. *Eur. J. Inorg. Chem.* **2009**, *2009*, 5358−5366.

(26) Carrington, S. J.; Chakraborty, I.; MAscharak, P. K. *Chem Commun.* **2013**, *49*, 11254−11256.

(27) (a) Vlček, A., Jr.; Farrell, I. R.; Liard, D. J.; Matousek, P.; Towrie, M.; Parker, A. W.; Grills, D. C.; George, M. W. *J. Chem. Soc.,*

Dalton Trans. **2002**, 701. (b) Farrell, I. R.; Vlček, A., Jr. *Coord. Chem. Rev.* **2000**, *208*, 87−101.
(28) Several examples of sixteen electron cationic metal complexes with weakly coordinating anions are present in the literature. See, for example, Beck, W.; Sünkel, K. *Chem. Rev.* **1988**, *88*, 1405−1421.
(29) (a) Scheiring, T.; Kaim, W.; Fielder, J. *J. Organomet. Chem.* **2000**, *598*, 136−141. (b) Carriedo, G. A.; Pérez-Martínez, J. A.; Miguel, D.; Riera, V.; García-Granda, S.; Pérez-Carreño, E. *J. Organomet. Chem.* **1996**, *511*, 77−84.
(30) (a) Blackmore, K. J.; Lal, N.; Ziller, J. W.; Heyduk, A. F. *Eur. J. Inorg. Chem.* **2009**, *2009*, 735−743. (b) Lionetti, D.; Medvecz, A. J.; Ugrinova, V.; Quiroz-Guzman, M.; Noll, B. C.; Brown, S. N. *Inorg. Chem.* **2010**, *49*, 4687−4697. (c) Lippert, C. A.; Soper, J. D. *Inorg. Chem.* **2010**, *49*, 3682−3684. (d) Heneline, M. R.; Clapp, L. A.; Hardcastle, K. I.; Soper, J. D. *Polyhedron* **2010**, *29*, 164−169.
(31) (a) Darensbourg, D. J.; Freolich, J. A. *J. Am. Chem. Soc.* **1977**, *99*, 5940−5946. (b) Behrens, H.; Lampe, R. J.; Merbach, P.; Moll, M. *J. Organomet. Chem.* **1978**, *159*, 201−217. (c) Uson, R.; Riera, V.; Gimeno, J.; Laguna, M. *Transition Met. Chem.* **1977**, *2*, 123−130.
(32) Palmer, G. T.; Basolo, F. *J. Am. Chem. Soc.* **1985**, *107*, 3122−3129.